# NADPH oxidase 2 limits amplification of IL-1β–G-CSF axis and an immature neutrophil subset in murine lung inflammation

Zhimin Song,[1] Sourav Bhattacharya,[1] Guangming Huang,[1] Zev J. Greenberg,[1] Wei Yang,[2] Juhi Bagaitkar,[3] Laura G. Schuettpelz,[1] and Mary C. Dinauer[1,4]

[1]Department of Pediatrics and [2]Department of Genetics, Washington University School of Medicine in St. Louis, St. Louis, MO; [3]Center for Microbial Pathogenesis, Abigail Wexner Research Institute at Nationwide Children's Hospital, The Ohio State University College of Medicine, Columbus, OH; and [4]Department of Pathology and Immunology, Washington University School of Medicine in St. Louis, St. Louis, MO

**Key Points**

- In CGD mice, fungal cell walls upregulate numbers of infiltrating neutrophils producing IL-1β to amplify a neutrophil pipeline via G-CSF.

- The amplified IL-1β–G-CSF axis in CGD mice promotes lung infiltration with increased numbers of proinflammatory immature neutrophils.

The leukocyte NADPH oxidase 2 (NOX2) regulates inflammation independent of its antimicrobial activity. Inherited defects in NOX2 lead to chronic granulomatous disease (CGD), associated with recurrent bacterial and fungal infections, often with excessive neutrophilic inflammation that results in significant inflammatory burden and tissue damage. We previously showed that excessive leukotriene B4 (LTB4) production by NOX2-deficient mouse neutrophils was a key driver of elevated lung neutrophil infiltration in the initial response to pulmonary challenge with the model fungal particle zymosan. We now identify interleukin-1β (IL-1β) and downstream granulocyte colony-stimulating factor (G-CSF) as critical amplifying signals that augment and sustain neutrophil accrual in CGD mice. Neutrophils, delivered into the lung via LTB4, were the primary source of IL-1β within the airways, and their increased numbers in CGD lungs led to significantly elevated local and plasma G-CSF. Elevated G-CSF simultaneously promoted increased granulopoiesis and mobilized the release of higher numbers of an immature CD101⁻ neutrophil subset from the marrow, which trafficked to the lung and acquired a significantly more proinflammatory transcriptome in CGD mice compared with wild-type mice. Thus, neutrophil-produced IL-1β and downstream G-CSF act sequentially but nonredundantly with LTB4 to deploy neutrophils and amplify inflammation in CGD mice after inhalation of zymosan. NOX2 plays a critical role in dampening multiple components of a feed-forward pipeline for neutrophil recruitment, and these findings highlight NOX2 as a key regulator of neutrophil number, subsets, and function at inflamed sites.

## Introduction

The leukocyte NADPH oxidase 2 (NOX2) is a multisubunit enzyme that generates superoxide, the precursor to reactive oxygen species that play crucial roles in microbial killing and downregulating the inflammatory response in both infectious and sterile inflammation.[1-3] Genetic defects in NOX2 lead to the primary immunodeficiency chronic granulomatous disease (CGD), accompanied by both recurrent

The full-text version of this article contains a data supplement.

infections and aberrant inflammation.[1] In CGD, some of the most debilitating infections involve opportunistic fungi such as *Aspergillus* species, which can cause life-threatening pneumonia often accompanied by exuberant neutrophil infiltration and abscess formation.[4-6] Even noninfectious fungal cell walls elicit excessive neutrophilic inflammation in CGD mice, associated with increased tissue levels of inflammatory cytokines.[7-10]

The pathogenesis of hyperinflammation in CGD is incompletely understood, but dysregulation of pathways controlling neutrophil number and function likely plays a central role. Neutrophils are major effectors of innate immunity and rapidly respond to signals generated in response to microbial invasion or noninfectious inflammation.[11,12] Balanced regulation of these responses is important to limit excessive neutrophil numbers at inflamed sites and prevent tissue damage or delayed resolution. Deployment of neutrophils to tissues is driven by local signals that promote their extravasation, and neutrophils themselves produce additional mediators upon arrival, setting into play feed-forward loops for additional recruitment.[12] Neutrophils actively alter their gene expression in response to local inflammatory signals, which includes their production of chemokines and other cytokines that amplify the inflammatory response.[12-17] Mediators produced at inflamed sites, most notably granulocyte colony-stimulating factor (G-CSF), also act systemically to mobilize release of neutrophils from the marrow storage pool into the blood as well as increase granulopoiesis.[11,18-20] In addition, recently identified phenotypic and functional heterogeneity among neutrophils at homeostasis and in response to microbes, inflammatory disease, and cancer[21-25] may provide an additional layer of regulation.

The loss of NOX2-derived reactive oxygen species affects multiple cellular processes involved in inflammatory responses.[1,3] For example, many studies have shown that CGD neutrophils and macrophages have increased NF-κB activation and proinflammatory gene transcription in response to various stimuli in vitro due to altered redox regulation of signaling proteins.[8,9,26-29] Interleukin-1 (IL-1) production and inflammasome activation are also increased in myeloid cells.[27,30-34] In neutrophils, increased calcium entry due to loss of electrogenic NOX2 activity results in excessive production of the chemoattractant leukotriene B4 (LTB4).[10,35,36]

Much less is known about how dysregulated cellular responses in CGD are co-opted to drive increased inflammation. However, insights into how lack of NOX2 deregulates control of neutrophil numbers and function are emerging. In damage-associated molecular pattern–induced peritonitis in CGD mice, increased local release of IL-1α by sentinel myeloid cells promotes an excessive G-CSF–regulated neutrophilic response.[34] Activated CGD neutrophils themselves boost inflammation after inhalation of the sterile fungal particle zymosan, where neutrophil infiltration into the lungs is markedly increased within hours by an amplified loop involving neutrophil LTB4 and its receptor BLT1.[10]

The goal of this study was to investigate whether additional inflammatory mediators are required for the overexuberant response to fungal cells in CGD lungs, hypothesizing that IL-1β may collaborate with LTB4 as part of a lipid mediator–cytokine cascade.[37] We found that IL-1β and downstream G-CSF were necessary to amplify and sustain neutrophilic recruitment into CGD lungs following zymosan challenge and that neutrophils delivered into the lung via LTB4 were the primary source of IL-1β within the airways. Moreover, because of increased numbers of IL-1β–positive lung neutrophils,

higher IL-1β levels in CGD mice led to significantly elevated local and plasma G-CSF in CGD mice compared with wild-type (WT) mice, accompanied by increased granulopoiesis and mobilization of greater numbers of immature neutrophils. The immature subset accounted for the major fraction of neutrophils trafficked to zymosan-inflamed lung in both WT and CGD mice but acquired a significantly more proinflammatory transcriptome in the latter. Thus, NOX2 plays a critical role in dampening multiple components of a feed-forward pipeline for recruiting neutrophils to inflamed sites.

## Materials and methods

### Mice

WT C57BL/6J mice were purchased from Jackson Laboratory (#000664) or bred in-house. Mice with inactivated X-linked *Cybb*[38] in C57BL/6J or B6.SJL-PtrcaPep3b/BoyJ[39] backgrounds were bred in-house. Mice were housed under specific pathogen-free conditions, and both sexes used between 10 and 14 weeks of age in experiments were approved by the Institutional Animal Care and Use Committee at Washington University, St. Louis.

### Zymosan-induced lung inflammation

Mice were challenged with 20 μg sterile zymosan by intranasal instillation and euthanized to analyze inflammation in bronchoalveolar lavage (BAL) and lung samples.[10] In some experiments, mice were administered zileuton (100 mg/kg) or vehicle by gavage, or injected IP with 0.5 mg of anti–IL-1β or isotype control antibodies (BioXcell), or 100 μg of anti–G-CSF antibody (Peprotech).[10,34] For RNA sequencing, lung single-cell suspensions[10] were stained as live (7-AAD-negative) CD45$^+$CD11b$^+$Ly6G$^+$ along with CD101, and sorted as CD45$^+$CD11b$^+$Ly6G$^+$CD101$^-$ or CD45$^+$CD11b$^+$Ly6G$^+$CD101$^+$ on the FACSAria Fusion cell sorter (BD).

### Statistics

Statistical analyses were performed using GraphPad Prism 9.0. Statistical significance was assessed by Student $t$ test or one-way analysis of variance (ANOVA) as indicated. $P < .05$ was considered significant.

Information on additional methods is provided in the supplement.

## Results

### CGD mice have more pro–IL-1β$^+$ neutrophils during zymosan-induced lung inflammation

Following zymosan inhalation, CGD mice displayed progressively higher numbers of BAL neutrophils and increasing lung infiltrates over the first 24 hours compared with WT mice (Figure 1A-B) (see also[10]). To assess potential sources of IL-1β in BAL, we used flow cytometry to identify pro–IL-1β$^+$ cells (supplemental Figure 1A). In naive WT and CGD mice, very few cells were pro–IL-1β$^+$ (Figure 1C and supplemental Figure 1B), which were primarily alveolar macrophages (supplemental Figure 1B-C). By 8 hours after the administration of zymosan, the percentage of BAL cells that were pro–IL-1β$^+$ increased markedly in both WT and CGD mice of which the majority were neutrophils (Figure 1C and supplemental Figure 1B-C). Overall, 30% to 50% of BAL neutrophils were pro–IL-1β$^+$ following zymosan challenge in WT and
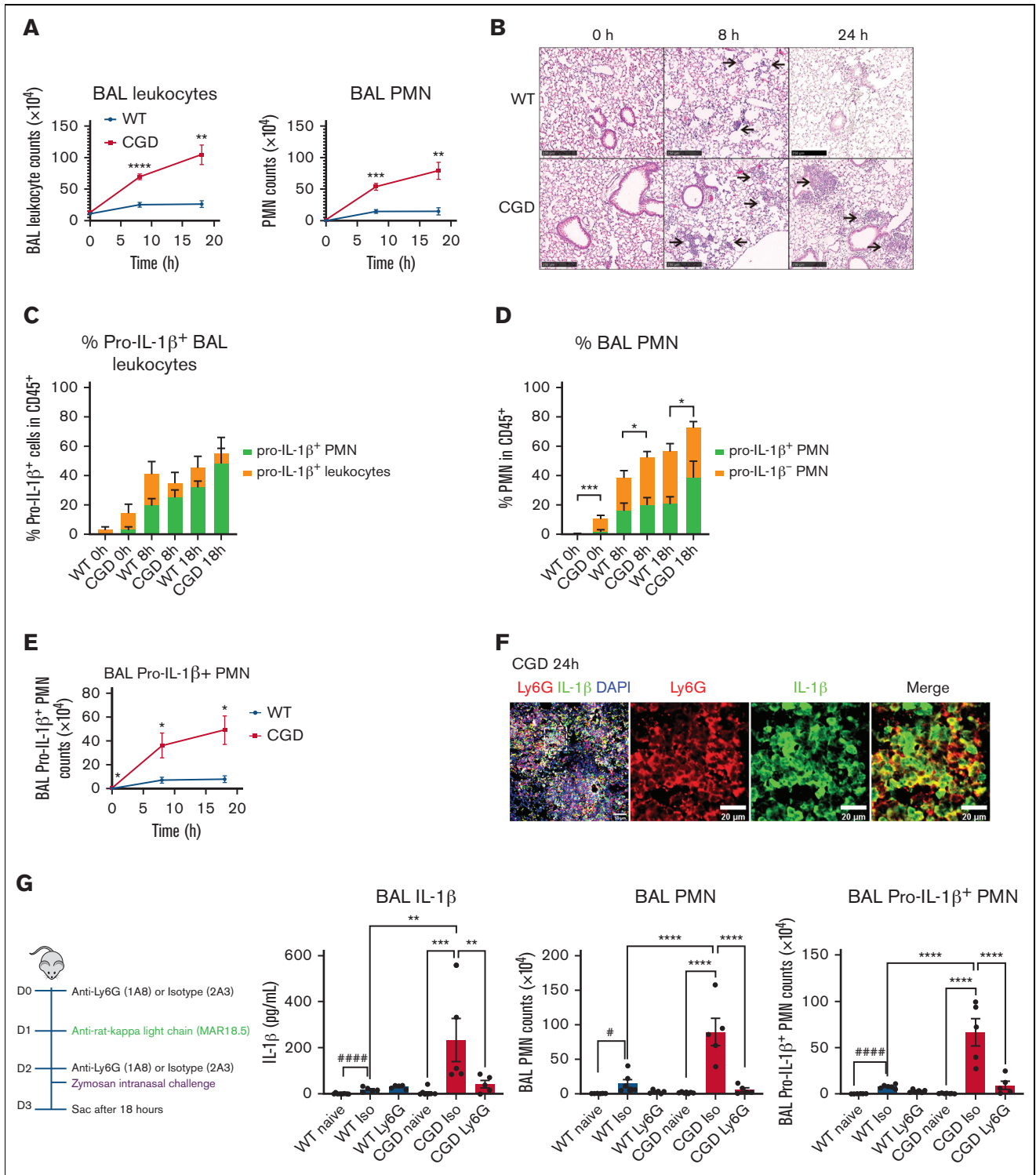
**Figure 1. Neutrophils are the major source of IL-1β in zymosan-induced lung inflammation in CGD mice.** WT and CGD mice were challenged with 20 μg intranasal zymosan. BAL and lung samples were collected at different time points. (A) Total leukocyte counts from 3 mL BAL fluid. The percentage of neutrophils were identified by cytospin and used to calculate BAL neutrophil (PMN) counts. (B) Formalin-fixed, paraffin-embedded lung sections were stained with hematoxylin and eosin. Scale bar, 250 μm. (C) Percentage of pro–IL-1β⁺ cells in CD45⁺ BAL leukocytes and the portion that are pro–IL-1β⁺ PMN calculated from flow cytometry results. (D) Percentage of BAL pro–IL-1β⁺ and pro–IL-1β⁻ PMN in CD45⁺ BAL leukocytes calculated from flow cytometry results. *, comparison between WT and CGD for the percentage of total PMN (both pro–IL-1β⁺ and pro–IL-1β⁻) in CD45⁺ leukocytes. (E) Total pro–IL-1β⁺ PMN counts in BAL were calculated from flow cytometry results. Panels C to E, n ≥ 6 in each group from >3 independent experiments. Data are means ± SEM. *$P < .05$; **$P < .01$; by Student $t$ test. (F) Immunofluorescence staining of formalin-fixed, paraffin-embedded lung sections with anti-Ly6G antibody, anti–IL-1β antibody, and 4′,6-diamidino-2-phenylindole. Scale bar, 50 μm or 20 μm. (G) WT and CGD mice were sequentially injected intraperitoneally

CGD mice (Figure 1D). However, the total number of pro–IL-1β+ BAL neutrophils were fourfold higher in CGD mice compared with WT by 8 hours and sevenfold higher at 18 hours (Figure 1E and supplemental Figure 1B). This largely reflected the much greater numbers of BAL neutrophils in CGD mice (Figure 1A) and the portion of pro–IL-1β+ leukocytes that were neutrophils (supplemental Figure 1C). The mean fluorescence intensity of pro–IL-1β+ in WT and CGD neutrophils was similar at 8 hours (not shown), but at 18 hours, was modestly but significantly increased in CGD neutrophils (mean fluorescence intensity values: WT 1777 ± 70.6; CGD 2251 ± 142.9; mean ± standard error of the mean, N ≥ 6, $P <$ .05). There was no significant difference between WT and CGD mice in the number of other pro–IL-1β+ myeloid cells (supplemental Figure 1B). In immunostained lung sections obtained from CGD mice at 24 hours after zymosan challenge, the majority of IL-1β+ cells in inflammatory foci were Ly6G+ (Figure 1F). Taken together, these results show that zymosan instillation induces accumulation of pro–IL-1β+ neutrophils in the inflamed lung but at substantially higher numbers in CGD compared with WT mice.

## Neutrophils are the major source of IL-1β in zymosan-induced lung inflammation in CGD mice

Next, we investigated whether neutrophils were the major source of BAL IL-1β in CGD mice. IL-1β BAL levels at 18 hours after zymosan inhalation were significantly increased from naive in both WT and, much more profoundly, in CGD (Figure 1G). Following anti-Ly6G administration, both total BAL neutrophils and those that were pro–IL-1β+ were significantly decreased at 18 hours in CGD mice after zymosan (Figure 1G). Moreover, neutrophil depletion significantly decreased IL-1β BAL levels in zymosan-challenged CGD mice (Figure 1G). Collectively, these results show that neutrophils were the major source of increased IL-1β in CGD BAL during the acute phase of zymosan-induced inflammation.

## Neutralization of IL-1β reduces zymosan-induced lung inflammation in CGD mice

To determine whether IL-1β played a role in zymosan-induced neutrophilic inflammation, we administered an IL-1β–blocking antibody before challenge. Whereas neutrophil infiltration into lungs of both WT and CGD mice in the first 8 hours is dependent on LTB4 synthesis,[10] blocking IL-β did not reduce BAL or lung neutrophils in either genotype at this time point (supplemental Figure 2A). Because zymosan-induced inflammation, including pro-IL-1β–positive neutrophils, plateaued in WT mice after 8 hours and remained much lower than in CGD mice (Figure 1), the impact of blocking IL-1β was not studied at later times in WT mice. However, anti–IL1-β markedly reduced lung inflammation in CGD mice at 24 hours, with significantly reduced total leukocytes and neutrophils in BAL (Figure 2A) Neutrophil numbers were also reduced in lung cell suspensions (Figure 2B), and lung parenchyma showed a profound decrease in neutrophil infiltrates (Figure 2C). We conclude that the significantly higher levels of IL-1β produced in the lungs of CGD mice are required to sustain the increase in zymosan-induced

inflammation. However, IL-1β does not significantly contribute to augmenting this response until after 8 hours, which differs from the strong dependency on LTB4 overproduction even during the first 8 hours.[10] This suggests that an LTB4–IL-1β cascade amplifies the neutrophilic inflammation in CGD mice.

## Neutralization of IL-1β reduces lung and plasma G-CSF levels at 24 hours in zymosan-challenged CGD mice

IL-1β/IL-1R signaling induces the expression of multiple proinflammatory mediators by hematopoietic and nonhematopoietic cells.[40,41] We focused on identifying IL-1β–regulated mediators produced in inflamed lung that could influence neutrophil responses. CXCL1, CXCL2, IL-6, and G-CSF transcripts in lung tissue were increased in CGD at 24 hours following zymosan challenge and significantly reduced by anti–IL-1β, especially Csf3 (G-CSF) (Figure 2D). In ELISAs of BAL samples, G-CSF levels were significantly reduced by IL-1β neutralization and IL-6 levels showed a trend for reduction, whereas IL-1β had less of a role on BAL CXCL1 and CXCL2 levels (Figure 2E). Because G-CSF is a major regulator of neutrophil biology, including basal and stress granulopoiesis, mobilization, and neutrophil priming,[11,19] we also examined G-CSF levels in the plasma. At 8 hours after zymosan challenge, plasma G-CSF levels rose substantially, which were modestly but significantly higher in CGD compared with WT mice (Figure 2F). Plasma G-CSF levels continued to rise in CGD mice over 24 hours (Figure 2F) but were significantly reduced by anti–IL-1β treatment (Figure 2F). We conclude that IL-1β is critical for increasing G-CSF levels not only in the lung but also in the plasma of CGD mice during this phase of zymosan-induced inflammation.

## G-CSF neutralization reduces zymosan-induced lung inflammation in CGD mice

Next, we established that blocking G-CSF was sufficient to dampen neutrophil accumulation in the lungs of CGD mice at 24 hours after zymosan challenge. We administered a neutralizing G-CSF antibody before zymosan, which significantly decreased inflammatory neutrophils in BAL and lung at 24 hours (Figure 3A-B), along with a marked reduction of focal neutrophil infiltrates in lungs (Figure 3C). Administration of anti–G-CSF did not blunt expression of Il6, Cxcl1, or Cxcl2 in zymosan-challenged lung (Figure 3D) and also did not affect BAL levels of IL-6 but, for uncertain reasons, increased CXCL1 and CXCL2 levels (Figure 3E). Collectively, these results establish G-CSF as a key downstream effector of IL-1β to promote zymosan-induced neutrophilic lung inflammation in CGD mice.

## CGD mice have expanded granulopoiesis in zymosan-induced lung inflammation

Because G-CSF is a key cytokine for activating demand granulopoiesis in response to inflammation or infection,[18,42,43] we used flow cytometry to analyze hematopoietic progenitor cells (HPCs)[44] and

---

**Figure 1 (continued)** with anti-Ly6G or isotype and anti-rat κ light chain, followed by intranasal instillation of 20 μg zymosan. After 18 hours, cells were counted from 3 mL BAL and cell composition analyzed by cytospin. IL-1β level in first milliliter of BAL was determined by ELISA. BAL PMN counts were calculated from cytospin results. BAL pro–IL-1β+ PMN counts were calculated from flow cytometry results. n ≥ 5 in each group from 2 independent experiments. Data are means ± SEM. **$P <$ .01; ***$P <$ .001; ****$P <$ .0001, by one-way ANOVA. For panel G, BAL data in naive and isotype-treated WT mice were compared by Student t test (#$P <$ .05 and ####$P <$ .0001). ELISA, enzyme-linked immunosorbent assay; SEM, standard error of the mean.
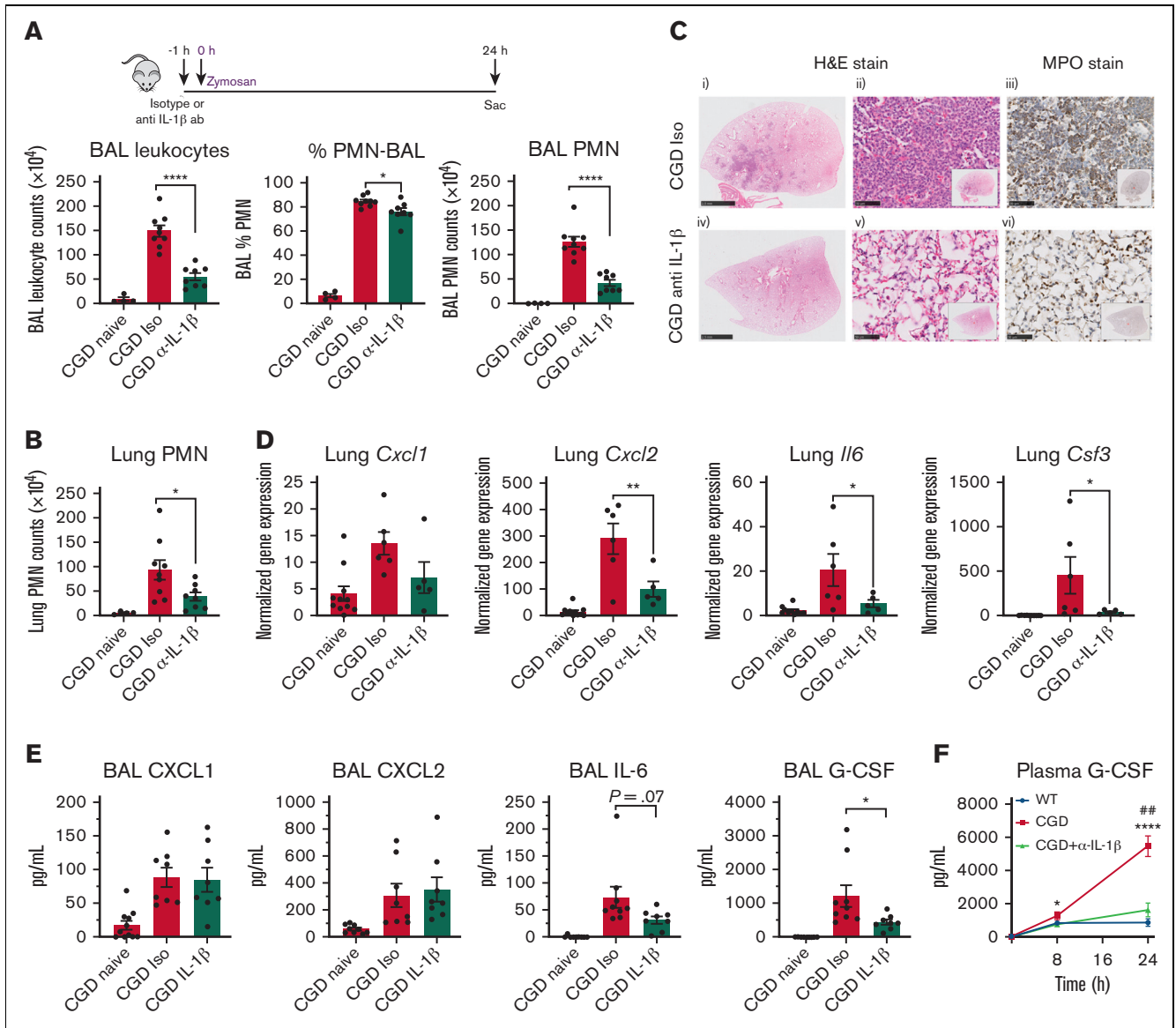
**Figure 2. IL-1β neutralization reduces zymosan-induced lung inflammation and G-CSF level in BAL in CGD mice at 24 hours.** (A-B) CGD mice were injected intraperitoneally with anti–IL-1β antibody or isotype, followed by intranasal instillation of 20 μg zymosan after 1 hour. BAL and lung tissue collected at 24 hours after zymosan challenge. (A) Total leukocyte counts from 3 mL BAL fluid. The percentage of neutrophils were identified by cytospin. BAL PMN counts were calculated from cytospin results. (B) PMN (CD45+CD11b+Ly6G+) counts from right lung inferior lobe were calculated by flow cytometry. Panels A and B, n ≥ 4 from >2 independent experiments. Data are means ± SEM. *$P < .05$, ****$P < .001$, by one-way ANOVA. (C) Formalin-fixed, paraffin-embedded lung sections were stained with hematoxylin and eosin or processed for immunohistochemical staining with MPO. Scale bar, 2.5 mm for (i) and (iv) and 50 μm for (ii), (iii), (v), and (vi). (D) Gene expression level of *Cxcl1*, *Cxcl2*, *Il6*, and *Csf3* from lung tissue were determined by qPCR. n ≥ 5 from 2 independent experiments. Data are means ± SEM. *$P < .05$, **$P < .01$, by one-way ANOVA. (E) CXCL1, CXCL2, IL-6, and G-CSF levels in first milliliter of BAL were determined by ELISA. n ≥ 8 from >3 independent experiments. Data are means ± SEM. *$P < .05$, by one-way ANOVA. (F) G-CSF level in plasma was determined by ELISA. n ≥ 5 from >3 independent experiments. Data are means ± SEM. *$P < .05$; ****$P < .0001$, ##$P < .01$; by Student *t* test; * indicates comparison between WT and CGD groups, # indicates comparison between CGD and CGD α-IL-1β antibody groups. qPCR, quantitative polymerase chain reaction; SEM, standard error of the mean.

neutrophil precursors[45] (supplemental Figure 3A-B). The fraction of marrow cells among different HPC or neutrophil precursors was not significantly different between naive and zymosan-challenged WT and CGD mice (supplemental Figure 3C-D), as we previously reported.[34] Total marrow cell numbers were also similar in naive WT and CGD mice (Figure 4A). After zymosan challenge, marrow cellularity significantly increased in CGD but not WT mice (Figure 4A), along with absolute numbers of primitive progenitor LSK cells and myeloid-

predominant progenitors (CMP, GMP, and MEP). With the exception of CMP, HPC numbers were also significantly greater in zymosan-challenged CGD mice compared with WT mice (Figure 4A). Zymosan-induced inflammation also triggered expansion of promyelocytes, myelocytes, and metamyelocytes in both WT and CGD mice, which again was significantly greater in CGD mice (Figure 4B). Altogether, these results show that marrow granulopoiesis expanded in both WT and CGD mice by 24 hours after zymosan challenge. This
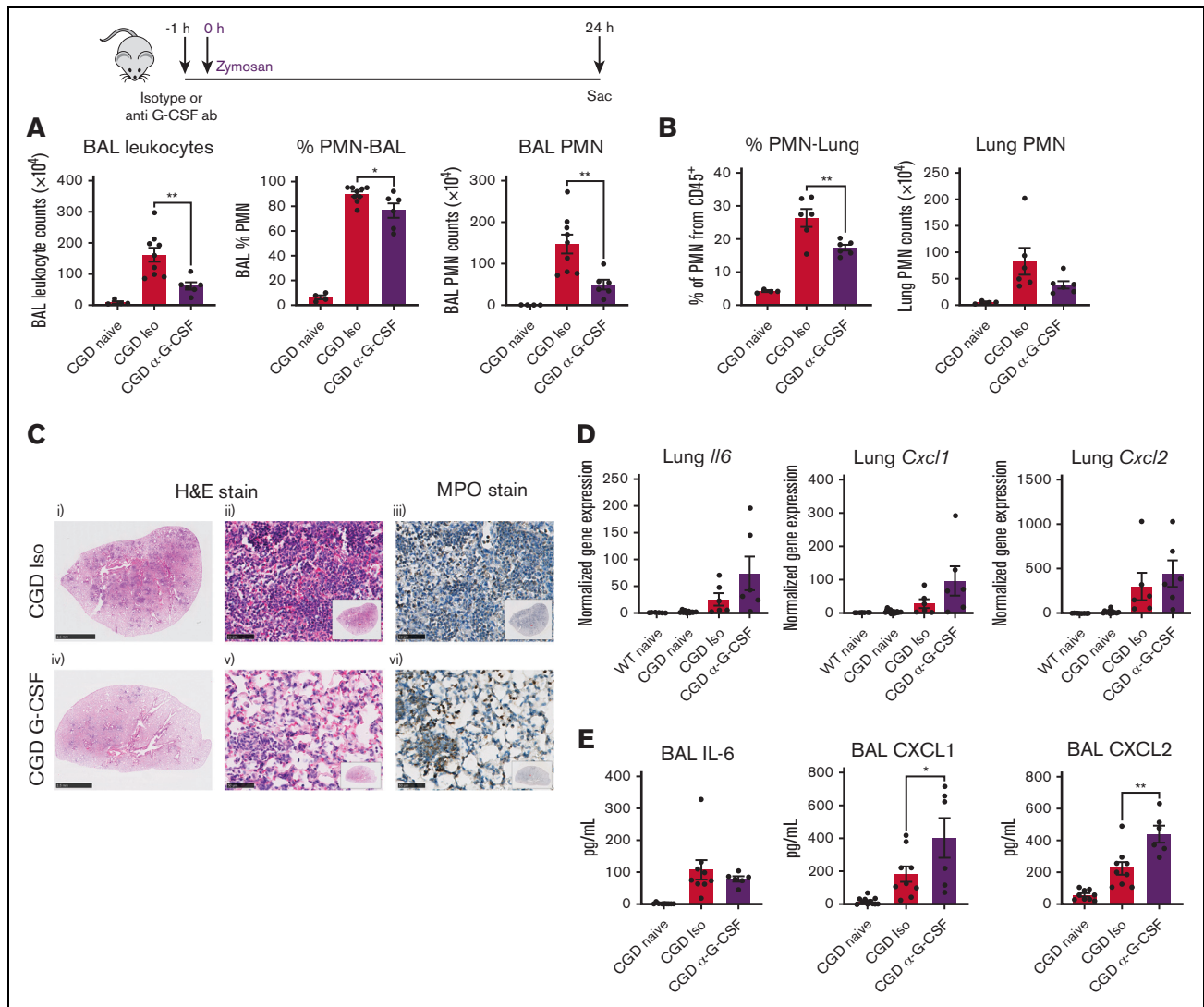
**Figure 3. G-CSF neutralization ameliorates zymosan-induced lung inflammation in CGD mice at 24 hours.** CGD mice were injected intraperitoneally with anti–G-CSF antibody or isotype, followed by intranasal instillation of 20 µg zymosan after 1 hour. BAL and lung tissue collected at 24 hours after zymosan challenge. (A) Total leukocyte counts from 3 mL BAL fluid. The percentage of neutrophils were identified by cytospin. BAL PMN counts were calculated by cytospin results. (B) Lung cells from the right inferior lobe were counted. Percentage of PMN was determined by flow cytometry, and PMN counts were calculated from flow cytometry results. n ≥ 4 from 2 independent experiments. (C) Formalin-fixed, paraffin-embedded lung sections were stained with hematoxylin and eosin or processed for immunohistochemical staining with MPO. Scale bar, 2.5 mm for (i) and (iv) and 50 µm for (ii), (iii), (v), and (vi). (D) Gene expression levels of *Il6*, *Cxcl1*, and *Cxcl2* from lung tissue were determined by qPCR. n ≥ 6 from 2 independent experiments. (E) IL-6, CXCL1, and CXCL2 levels in first milliliter of BAL were determined by ELISA. n ≥ 6 from 2 independent experiments. Data are means ± SEM. *$P < .05$; **$P < .01$, by one-way ANOVA. qPCR, quantitative polymerase chain reaction; SEM, standard error of the mean.

expansion was substantially more profound in CGD mice, consistent with their increased lung inflammation.

## CGD mice have neutrophilia and increased numbers of CD101⁻ immature neutrophils in marrow, blood, and lung at 24 hours after zymosan challenge

Infectious or sterile inflammation can evoke G-CSF–dependent mobilization of mature and immature neutrophils from marrow into peripheral blood, which then infiltrate into inflamed tissue.[15,17,18,46] To track neutrophil maturation status after lung zymosan challenge, we used flow cytometry to identify CD101 (supplemental Figure 4), a glycoprotein present on mature mouse neutrophils but absent on

earlier precursors.[16,46] These include a nonproliferating pool that have acquired gene signatures for key neutrophil functions but still have an immature nuclear morphology.[15,17,46] The CD101-negative (CD101⁻) immature neutrophil subset account for a substantial fraction of neutrophils that mobilize with G-CSF and migrate into inflammatory sites.[16,46]

We assessed neutrophil numbers and their maturation state based on their CD101 expression in marrow and the periphery in WT and CGD mice, both at homeostasis and after lung challenge with zymosan. At 24 hours after challenge, CGD but not WT mice had significant neutrophilia (Figure 5A). In naive WT and CGD mice, approximately two-thirds of Ly6G⁺CD11b⁺ neutrophils in the marrow were CD101⁻
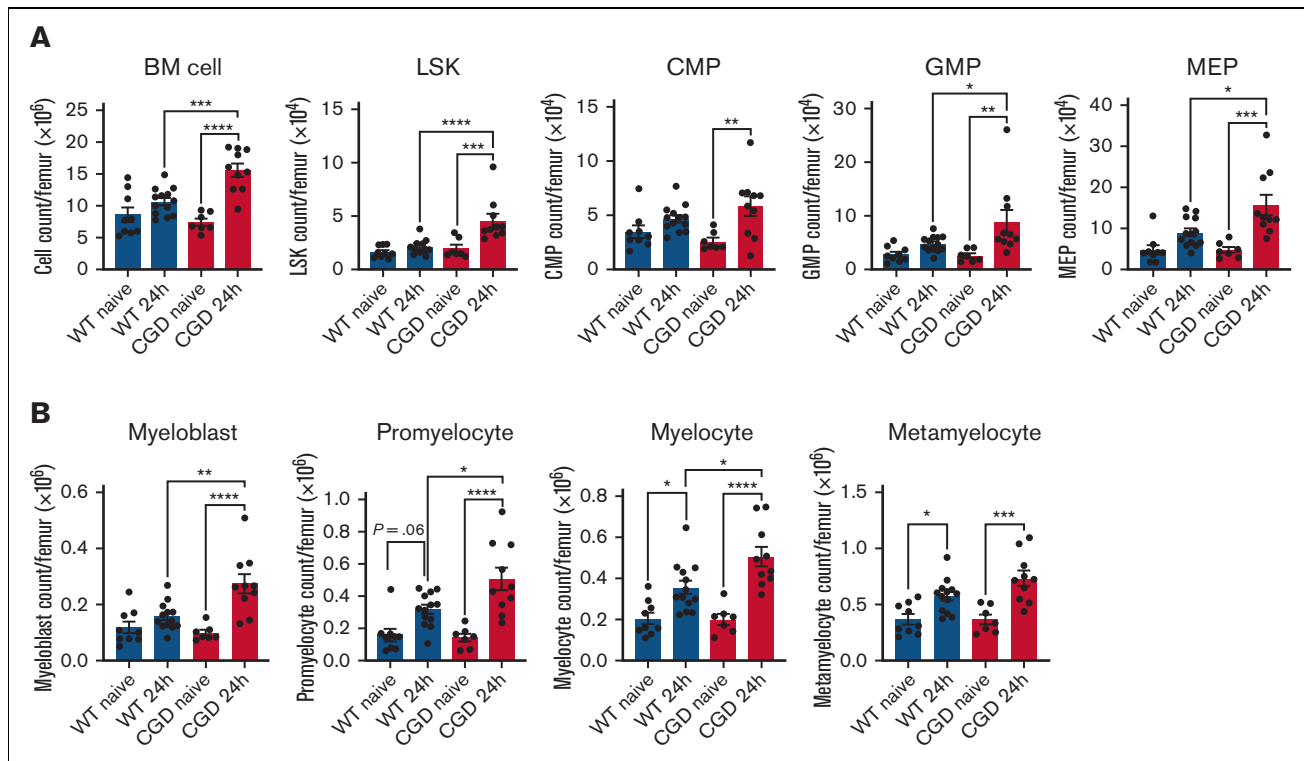
**Figure 4. CGD mice have expanded granulopoiesis compared with WT mice in zymosan-induced lung inflammation at 24 hours.** WT and CGD mice were challenged with 20 μg intranasal zymosan. BM cells were collected after 24 hours and analyzed by flow cytometry. (A) BM cells per femur were counted. LSK, CMP, GMP, and MEP counts were calculated from flow cytometry results. (B) Cell counts of myeloblast, promyelocyte, myelocyte, and metamyelocyte were calculated from flow cytometry results. n ≥ 7 from 3 independent experiments. Data are means ± SEM. *$P < .05$; **$P < .01$; ***$P < .001$; ****$P < .0001$, by one-way ANOVA. BM, bone marrow; CMP, common myeloid progenitors; GMP, granulocyte-macrophage progenitor; LSK, Lin⁻Sca1⁺c-Kit⁺; MEP, megakaryocyte-erythrocyte progenitor.

(Figure 5B-C) but very few immature neutrophils were found in peripheral blood (Figure 5D-E). CD101⁻neutrophils in marrow increased modestly at 24 hours after zymosan challenge, but the peripheral blood showed substantial increases in the relative fraction and number of immature neutrophils, which was significant in CGD mice (Figure 5B-E). The neutrophilia in zymosan-challenged CGD mice almost entirely reflected an increase in immature neutrophils, which accounted for approximately half of blood neutrophils at 24 hours (Figure 5E). Immature neutrophils were also found in the BAL after zymosan challenge, and compared with WT mice, CGD mice had approximately threefold higher fraction of this subset, accounting for almost two-thirds of BAL neutrophils (Figure 5F). Finally, the majority of lung neutrophils in both WT and CGD mice at 24 hours after zymosan were CD101⁻, and this fraction was again significantly higher in CGD (Figure 5G). We conclude that zymosan challenge induced a significant increase in the CD101⁻ immature neutrophil subset in the marrow and, especially, in the peripheral blood and inflamed lung, which were significantly higher in CGD mice compared with WT mice.

## Expansion of granulopoiesis and numbers of immature neutrophils in peripheral blood during zymosan-induced lung inflammation in CGD are driven by G-CSF and upstream IL-1β and LTB4

Next, to link the increased levels of G-CSF induced by lung inflammation in CGD mice to the expansion of granulopoiesis and

mobilization of immature neutrophils, we measured the effect of blocking G-CSF activity. Primitive LSK progenitors and MEP myeloid progenitors were significantly reduced by G-CSF blockade compared with isotype controls, along with a trend for decreased CMP (Figure 6A). There was a significant reduction in metamyelocytes as well as a trend of reduced numbers of promyelocytes and myelocytes (Figure 6B). Finally, G-CSF neutralization significantly reduced both percentage and absolute numbers of peripheral blood neutrophils after zymosan challenge, particularly immature CD101⁻ neutrophils (Figure 6C-D).

We also examined the effect of inhibiting 2 key upstream mediators, IL-1β (Figure 2) and LTB4,[10] using an IL-1β–blocking antibody or inhibiting LTB4 synthesis with zileuton. The results were similar to effects of neutralizing G-CSF. Inhibiting LTB4 synthesis or blocking IL-1β before zymosan challenge significantly decreased the number of marrow LSK, MEP, GMP, promyelocyte, and myelocytes as compared with control groups (supplemental Figure 5A-B). Peripheral blood immature neutrophils were also significantly decreased, along with a trend for reduced total blood neutrophil numbers in zileuton-treated mice (supplemental Figure 5A-D). In addition, we showed that inhibiting LTB4 synthesis significantly reduced the numbers of pro-IL-1β–positive BAL neutrophils at 8 hours and attenuated the increase in plasma G-CSF at both 8 and 24 hours after zymosan (supplemental Figure 5E-G). Collectively, these results demonstrate that the increased marrow granulopoiesis and mobilization of CD101⁻immature neutrophils
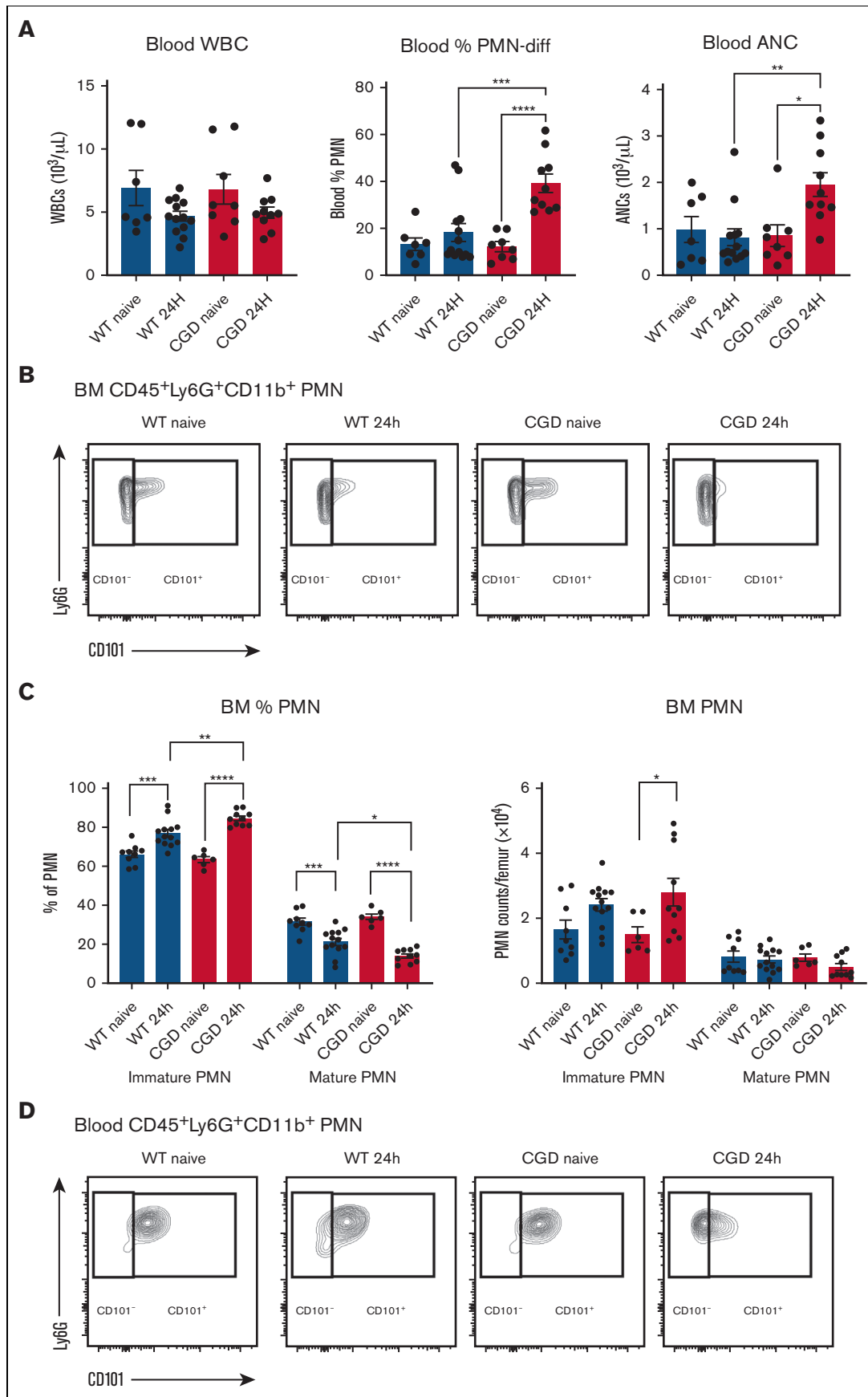
**Figure 5. CGD mice have increased percentage of CD101⁻ immature neutrophils in BM, blood, and lung in zymosan-induced lung inflammation at 24 hours.** WT and CGD mice were studied at baseline (naive) and 24 hours after challenged with 20 μg intranasal zymosan, as indicated. (A) Total WBCs, percentage of neutrophils, and
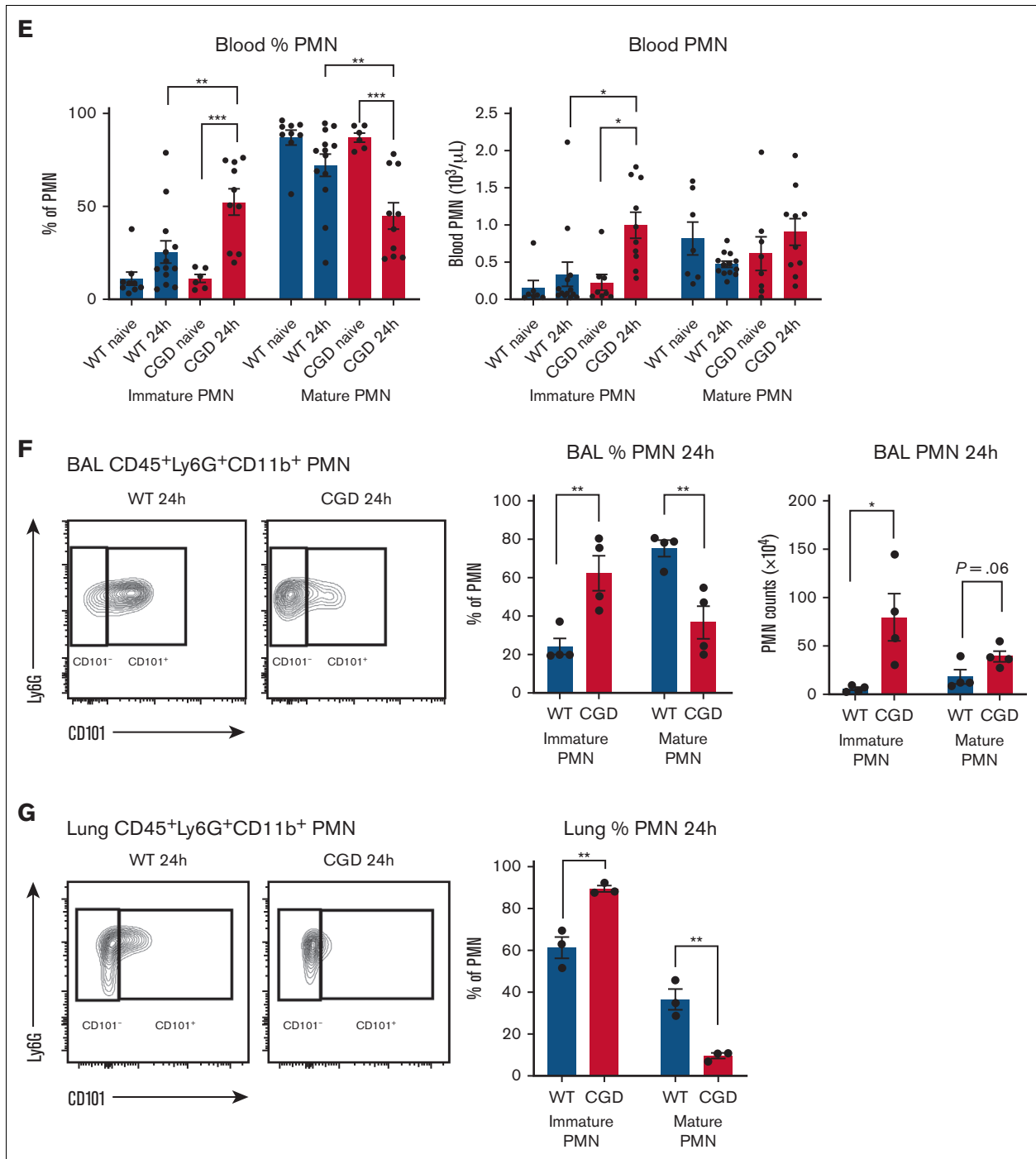
**Figure 5 (continued)** ANC were determined in peripheral blood by complete blood count and differential. (B) Representative flow cytometry of BM shows CD101⁻ PMN (CD45⁺CD11b⁺Ly6G⁺CD101⁻) and CD101⁺ PMN (CD45⁺CD11b⁺Ly6G⁺CD101⁺). (C) Percentage of CD101⁻ PMN and CD101⁺ PMN in BM determined by flow cytometry and BM cells counted per femur. BM CD101⁻ PMN and CD101⁺ PMN counts were then calculated using flow cytometry results. (D) Representative flow cytometry of peripheral blood shows CD101⁻ PMN (CD45⁺CD11b⁺Ly6G⁺CD101⁻) and CD101⁺ PMN (CD45⁺CD11b⁺Ly6G⁺CD101⁺). (E) Blood CD101⁻ PMN and CD101⁺ PMN were determined by flow cytometry. ANC were determined in peripheral blood by complete blood count and differential. Blood CD101⁻ PMN and CD101⁺ PMN counts were calculated from flow cytometry results. Panels A to E, n ≥ 6 from 3 independent experiments. Data are means ± SEM. *$P < .05$; **$P < .01$; ***$P < .001$; ****$P < .0001$, by one-way ANOVA. (F) Representative flow cytometry of CD101⁻ PMN and CD101⁺ PMN in BAL from zymosan-challenged mice at 24 hours. Percentage of CD101⁻ PMN and CD101⁺ PMN in BAL was determined by flow cytometry and used to calculate total BAL PMN in the 2 groups based on leukocyte counts from 3 mL BAL fluid. n = 4 from 2 independent experiments. Data are means ± SEM. *$P < .05$; **$P < .01$; by Student $t$ test. (G) Representative flow cytometry for CD101⁻ PMN and CD101⁺ PMN in zymosan-challenged mice in total lung cell suspensions at 24 hours. Percentage of CD101⁻ PMN and CD101⁺ PMN in lung was determined by flow cytometry. n = 3, data are means ± SEM. **$P < .01$, by one-way ANOVA. ANC, absolute neutrophil count; WBC, white blood cell.
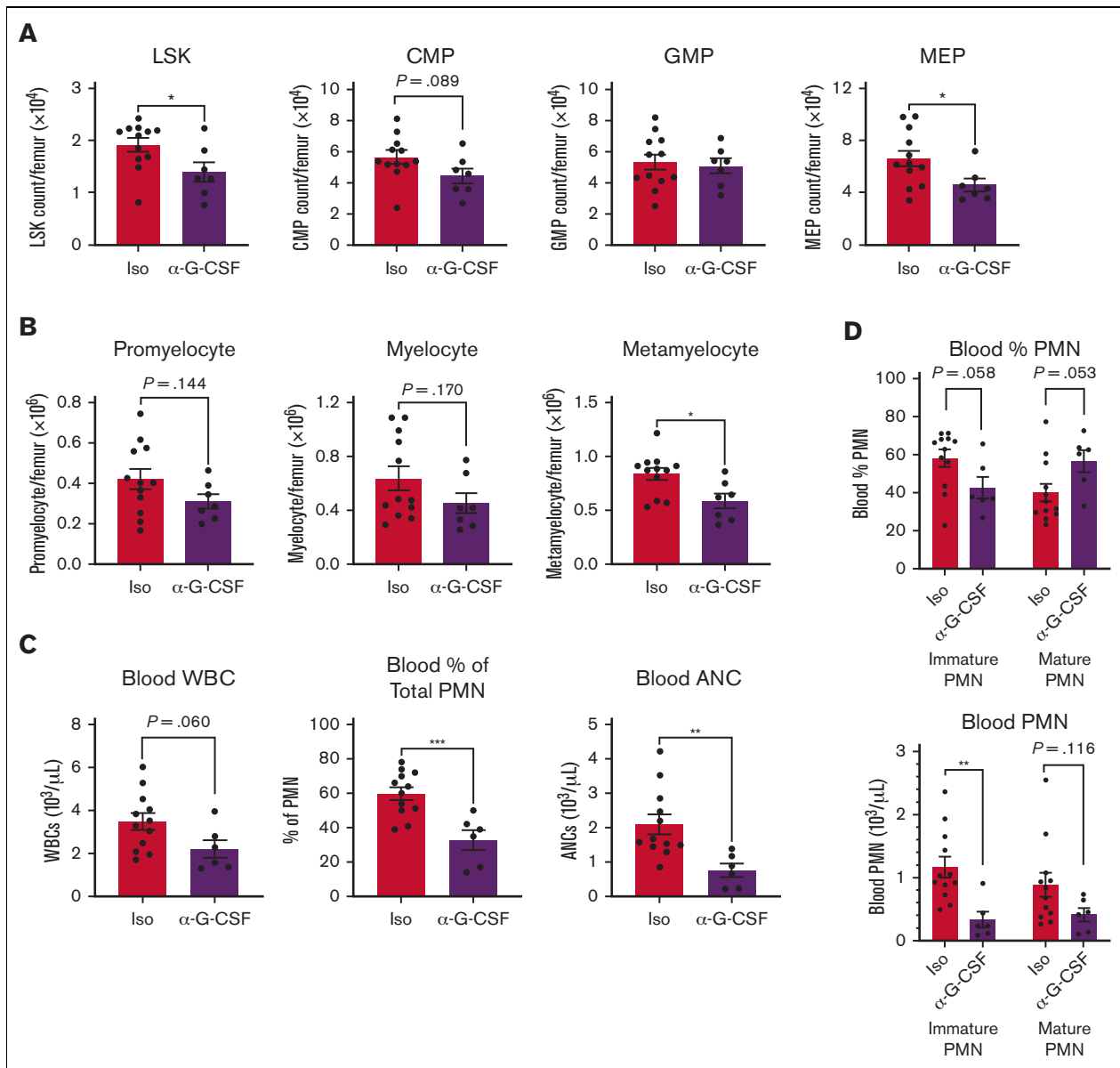
**Figure 6. G-CSF neutralization decreases granulopoiesis and peripheral blood immature neutrophils in zymosan-induced lung inflammation in CGD mice at 24 hours.** (A-D) CGD mice were injected intraperitoneally with anti–G-CSF antibody or isotype, 1 hour before zymosan challenge. BM cells were counted per femur. (A) LSK, GMP, CMP, and MEP counts per femur were calculated using flow cytometry results. (B) Cell counts of promyelocyte, myelocyte, and metamyelocyte were calculated using flow cytometry results. (C) Total WBC, percentage of PMN, and ANC were determined in peripheral blood by complete blood count and differential. (D) Blood immature CD101$^-$ PMN and CD101$^+$ mature PMN were determined by flow cytometry. Blood immature PMN and mature PMN counts were calculated by flow cytometry results. n $\geq$ 5 from >3 independent experiments. Data are means $\pm$ SEM. *$P < .05$; **$P < .01$; ***$P < .001$; by Student $t$ test. ANC, absolute neutrophil count; WBC, white blood cell.

into the peripheral blood of CGD mice during zymosan-induced lung inflammation is regulated via LTB4 and IL-1β–G-CSF–dependent signals.

## CGD CD101$^-$ neutrophils exhibit an increased proinflammatory transcriptomic profile

To gain insights into how the CD101$^-$ neutrophil subset compares with mature neutrophils in the lungs of WT and CGD mice at homeostasis and during inflammation, we profiled gene expression in sorted lung neutrophils using RNA sequencing. Multidimensional scaling analysis showed that gene expression signatures shifted for neutrophils in inflamed lungs compared with naive mice (Figure 7A). There were also differences between WT and CGD lung neutrophils after zymosan challenge, with a particularly distinct profile for CD101$^-$ immature neutrophils from inflamed CGD lung (Figure 7A). Differences among groups are also depicted in the Venn diagrams in Figure 7B-D and in a heatmap of the top 500 most variable genes (Figure 7E; supplemental Table 1). A far greater number of genes were differentially expressed between CGD and WT inflammatory lung neutrophils compared with those from naive mice (Figure 7B). In addition, there were many more
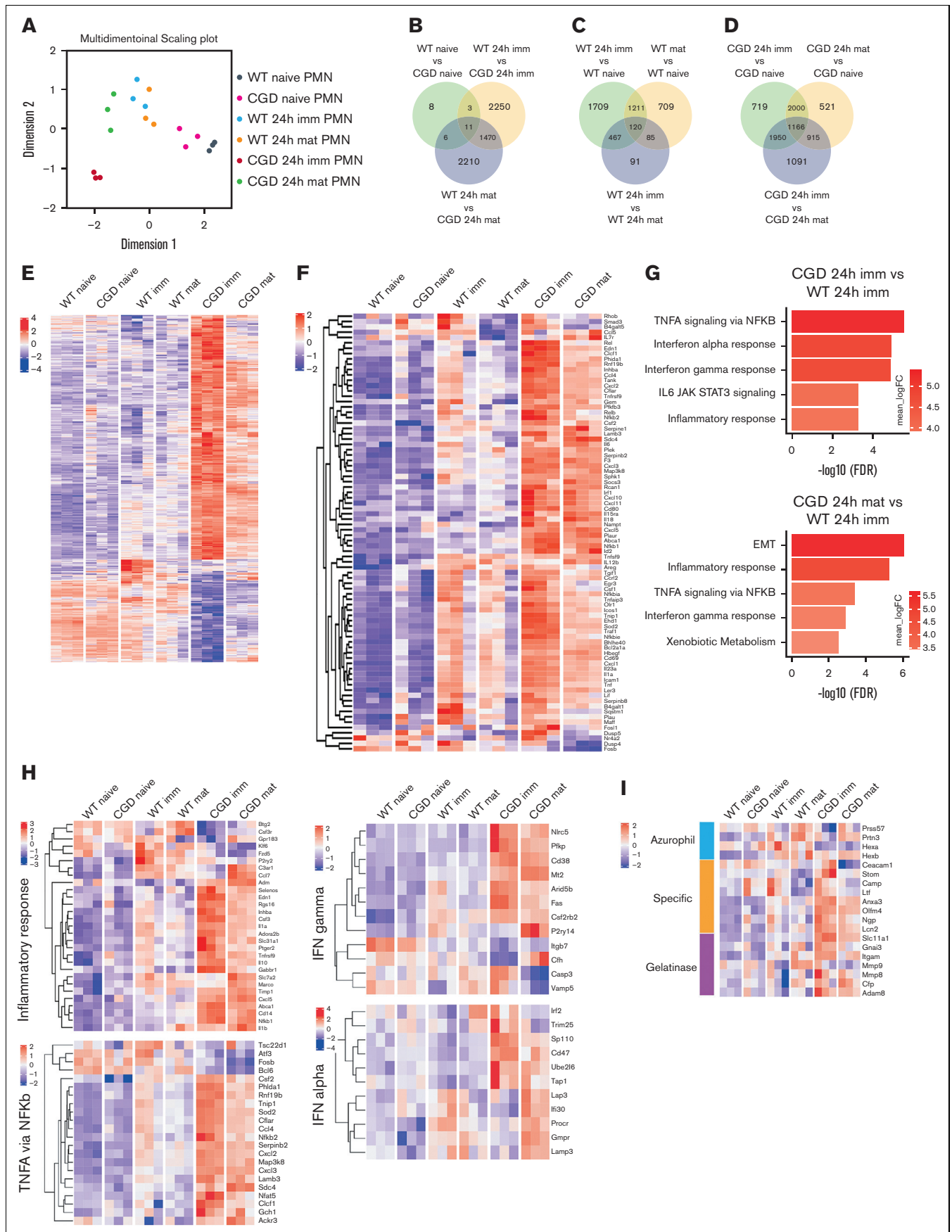
**Figure 7.**

genes differing in expression between immature and mature inflammatory lung neutrophils from CGD mice compared with WT mice (Figure 7C-D).

We used generally applicable gene-set enrichment analysis[47] of hallmark gene sets[48] to interrogate differences among groups. Both WT and CGD lung neutrophils isolated 24 hours after zymosan exhibited a more proinflammatory transcriptome compared with naive mice, with the tumor necrosis factor α (TNF-α) signaling via NF-κB and inflammatory response gene sets among the most significantly upregulated in both genotypes and in both CD101⁻ and CD101⁺ neutrophil subsets (supplemental Figure 6A-D). This activation is consistent with elevated TNF-α (supplemental Figure 6E), IL-1β, and other cytokines[10] in BAL. Expression of genes in the TNF-α signaling set was also significantly higher for both genotypes in CD101⁻ than in CD101⁺ neutrophils (Figure 7F and supplemental Figure 6A-B), and included *Tnf* itself, *Csf1*, *Icam1*, and various chemokines. Comparing expression profiles between WT and CGD inflammatory neutrophil subsets showed that TNF-α signaling, inflammatory response, and interferon response gene sets were significantly upregulated in CGD compared with WT Figure 7G). A heatmap highlights genes from these hallmark sets with significantly different expression between the various groups (Figure 7H). These include proinflammatory cytokines (*Csf2*, *Csf3*), chemoattractants (*Cxcl2*, *Cxcl3*, *Ccl4*), and transcription regulators (*Nfkb1*, *Nfkb2*, *Arid5b*, *Irf2*), as more highly expressed in CGD neutrophils, especially immature neutrophils.

In additional analyses, CD101⁻ neutrophils from inflamed lung exhibited higher expression of many granule transcripts, consistent with immaturity (Figure 7I). Genes related to IL-1β production and release were also more highly expressed in both mature and immature CGD inflammatory lung neutrophils compared with WT (supplemental Figure 6F).

We conclude that after zymosan, neutrophils in the inflamed lung have a more proinflammatory gene signature compared with lung neutrophils at steady state. Moreover, the transcriptome of CD101⁻ immature neutrophils, which account for the majority of neutrophils in the inflamed lung at 24 hours, is even more upregulated than mature neutrophils for genes associated with acute inflammation. Finally, the profiles in CGD neutrophils, although involving changes in the same gene sets as WT, are significantly more upregulated, which may contribute to the development of the hyperinflammation.

## Discussion

In this study, we established that an amplified IL-1β–G-CSF axis plays a nonredundant role in the exaggerated zymosan-induced inflammatory response in CGD mice and was necessary for sustaining neutrophilic lung inflammation beyond the first 8 hours. Although increased IL-1β has been previously implicated in pathogenesis of chronic inflammation in CGD,[30-34] to our knowledge, this study shows for the first time that IL-β produced by CGD neutrophils is part of an LTB4-initiated cascade elicited by exposure to fungal cell walls and that G-CSF is a key downstream collaborator. These results reinforce the importance of lipid mediator–cytokine cascades in the acute inflammatory response[37,49] and show how their dysregulation in the absence of NOX2 can lead to excessive neutrophil recruitment. Furthermore, our study also provides new insights into the heterogeneity of neutrophil responses during acute inflammation. An immature subset with a more proinflammatory transcriptional profile accounted for a major fraction of neutrophils in the inflamed lungs in both WT and CGD mice, which were present in larger numbers in CGD. Thus, at multiple points, CGD neutrophils themselves participate in amplifying a feed-forward pipeline for neutrophil recruitment and tissue inflammation in the response to fungal cell wells, resulting in exuberant inflammation in the absence of NOX2.

Although macrophages are classically considered to be the predominant source of the potent apical cytokine IL-1β,[40,41] there is an emerging recognition of the contribution of neutrophils to and impact of neutrophils on IL-1β production in both infectious processes and sterile inflammation.[49-55] Aforementioned prior studies with data similar to our findings show that neutrophils are a key and nonredundant source of IL-1β in the acute phase of the response. Although other myeloid cells can produce more IL-1β per cell, far more neutrophils can be recruited to inflammatory sites; thus, neutrophil-derived IL-1β can be of great importance for inducing downstream inflammatory mediators.[13] This may be especially problematic in the response to zymosan in CGD, where neutrophil recruitment is already amplified by increased LTB4. Our study does not address how pro–IL-1β is processed and released, which in neutrophils include a nonlytic inflammasome-dependent pathway as well as others.[56-58] However, activated CGD neutrophils have increased transcription of IL-1β and various proteins that promote its processing and secretion compared with WT neutrophils (supplemental Figure 6F; see also[27]), and LTB4 itself can promote increased *Il1b* transcription and inflammasome activation.[59] Hence, multiple factors that are dysregulated in neutrophils lacking NOX2 activity may contribute to excessive levels of IL-1β in the response of CGD mice, although the far greater number of neutrophils recruited to the inflamed tissue may play a dominant role.

Whereas IL-1–IL-1R signaling induces expression of multiple inflammatory mediators, we identified G-CSF as the major effector of IL-1β that promoted zymosan-induced lung inflammation in CGD mice. Of

**Figure 7. Transcriptomic analysis shows distinct expression signatures of lung neutrophils between WT and CGD mice.** (A) Multidimensional scaling plot of samples based on their gene expression. (B-D) Venn diagram of number of DEGs in the indicated groups (false discovery rate < 0.05). Genes in overlapping sets show differences in expression of 2 or 3 comparison pairs. (E) Heatmap of the relative expression of all groups for the top 500 DEGs between immature CD101⁻ PMN from inflamed WT and CGD lungs. Gene names are listed in supplemental Table 1. (F) Heatmap showing expression of lung PMN genes (limma-/voom-normalized) from hallmark gene sets (TNFA via NFKb) with significantly different expression between naive and inflamed lung or between CD101⁻ and CD101⁺ PMN in either WT or CGD. (G) Hallmark gene sets analyzed using GAGE for the indicated comparison pairs. (H) Heatmap showing expression of genes (limma-/voom-normalized), selected from indicated hallmark gene sets and chosen because they had significantly different expression in each of the following comparisons of inflammatory lung neutrophils: CGD CD101⁻ PMN vs WT CD101⁻ or CD101⁺ PMN, CGD CD101⁺ vs WT CD101⁻ or CD101⁺ PMN; and CGD CD101⁻ PMN vs CGD CD101⁺ PMN. (I) Expression of genes (limma-/voom-normalized) related to neutrophil granule production in the indicated groups of mice. ANC, absolute neutrophil count; DEG, differentially expressed gene; GAGE, generally applicable gene-set enrichment; MDS, multidimensional scaling.

note, neutralizing either IL-1β or G-CSF substantially ameliorated lung inflammation without reducing airway levels of CXCL1 or CXCL2, important neutrophil chemoattractants in the host response to fungal cell walls.[60,61] It is also important to note that prior studies in our mouse CGD model established that NOX2 deficiency per se does not enhance sensitivity to G-CSF–induced mobilization.[34] Increased G-CSF production in nonhematopoietic and hematopoietic cells can be induced by proinflammatory cytokines, including IL-1, IL-6, and TNF-α,[11,18,19] and CGD neutrophils in zymosan-inflamed lung, which have increased *Csf3* transcripts (Figure 7H), might themselves contribute to the increased G-CSF levels. Only a few studies have directly established a link between IL-1 and G-CSF for demand-adapted granulopoiesis in the acute response to inflammation. These include studies in mice in which alum, trauma, or *Candida* infection triggered emergency granulopoiesis and mobilization of immature neutrophils into the blood via IL-1R–dependent induction of G-CSF.[42,62,63] Our results further demonstrate a key role for IL-1–dependent G-CSF production to sustain delivery of neutrophils in response to fungal pathogen-associated molecular patterns in CGD mice, although it contributes to overexuberant inflammation. Finally, our study does not exclude that G-CSF could also aggravate the inflammation in CGD mice by priming neutrophil functions, such as enhancing adhesion or proinflammatory transcription via the Jak-Stat pathway.[11,19]

Neutrophils undergo proinflammatory transcriptional reprogramming when activated, with increased expression of genes encoding chemokines, cytokines, and other proteins important for the inflammatory process.[13] Our study showed that whereas similar groups of genes are differentially expressed in neutrophils from inflamed lung in WT and CGD mice compared with lung neutrophils from naive mice, the inflammatory gene signatures were significantly more upregulated in CGD neutrophils. Similar findings were reported in the K/BxN serum-transfer arthritis model, where more neutrophils with greater expression of proinflammatory gene sets accumulated in arthritic joints of CGD mice compared with WT.[64] These differences at least in part reflect a higher level of neutrophil activation because of increased local inflammation in CGD. However, CGD neutrophils activated in vitro with fungal pathogen-associated molecular patterns or Toll-like receptor ligands have increased gene transcription through amplified NF-κB and Jun/AP1 pathways,[8,27,28] indicating that cell-intrinsic hyper-reactivity in the absence of NOX2 activity could also play a role.

Finally, our findings provide new insights into the still-emerging understanding of neutrophil heterogeneity and responses during acute inflammation. The stage of neutrophil maturation can be an important determinant of phenotypic heterogeneity. Recent studies in humans and mice have used cell surface markers correlating with maturity, including CD16 and CD101, to examine neutrophil subsets in inflammation or in the tumor microenvironment.[16,23,46,65-70] For example, immature CD16^{dim}-banded human neutrophils mobilized in response to endotoxin had higher bactericidal capacity.[66] A striking finding in our study was that more than half of neutrophils present in the inflamed lungs of WT and CGD mice were CD101^{−} and had a more proinflammatory gene profile than their mature counterparts in the inflamed lung. To our knowledge, this is the first report of a differential transcriptional response by immature neutrophils, a subset that is rapidly mobilized in response to infection and inflammation and which may be endowed with enhanced functionality to respond to threats. The proinflammatory transcriptome was even more skewed in CGD CD101^{−} neutrophils, which illustrates how functional neutrophil heterogeneity can be affected by disorders of immune dysregulation and could contribute to aberrant inflammation.

In summary, our data advance understanding of how the absence of NOX2 deregulates feedback amplification of neutrophil recruitment and function at inflamed sites. Although neutrophil production of LTB4, chemokines, and cytokines facilitates a rapid response to sites of infection and injury, in the setting of CGD, some of these feedback loops are inappropriately amplified, leading to increased levels of LTB4 and IL-1β–G-CSF in zymosan-induced lung inflammation. This not only promotes acute inflammation but might also contribute to chronic inflammatory complications. Antagonism of IL-1 has already been proposed as a possible strategy to mitigate inflammation in patients with CGD,[30-32] and our study suggests that recently developed G-CSF receptor antagonists[71-73] could be considered. Our findings also provide new insights into the biological implications of neutrophil heterogeneity during acute inflammation, and higher numbers of a proinflammatory CD101^{−} neutrophil subset recruited to the lung may contribute to the increased inflammation in CGD. Targeting this subset could be an additional approach to ameliorate CGD hyperinflammation. Thus, the results demonstrate the importance of NOX2 in limiting excessive numbers of neutrophils at inflamed sites.

## Authorship

Contribution: Z.S., L.G.S., and M.C.D. designed the research; Z.S., S.B., G.H., Z.J.G., and W.Y. performed and/or analyzed the results of the experiments; W.Y. prepared the figures for the RNA sequencing data; Z.S. prepared the other figures; and Z.S. and M.C.D. wrote the manuscript with the input from J.B., L.G.S., S.B., and Z.J.G.

Conflict-of-interest disclosure: The authors declare no competing financial interests.

ORCID profiles: Z.S., 0000-0001-7977-2158; S.B., 0000-0002-2101-4124; Z.J.G., 0000-0002-6234-7005; W.Y., 0000-0001-8162-033X; J.B., 0000-0001-6185-1915; L.G.S., 0000-0001-6047-3641; M.C.D., 0000-0002-7796-2908.

Correspondence: Mary C. Dinauer, Washington University School of Medicine, 660 S. Euclid Ave, PO Box 8208, St. Louis, MO 63110; email: mdinauer@wustl.edu.

# References

1. Dinauer MC. Inflammatory consequences of inherited disorders affecting neutrophil function. *Blood*. 2019;133(20):2130-2139.

2. Nauseef WM. The phagocyte NOX2 NADPH oxidase in microbial killing and cell signaling. *Curr Opin Immunol*. 2019;60:130-140.

3. Zeng MY, Miralda I, Armstrong CL, Uriarte SM, Bagaitkar J. The roles of NADPH oxidase in modulating neutrophil effector responses. *Mol Oral Microbiol*. 2019;34(2):27-38.

4. Henriet S, Verweij PE, Holland SM, Warris A. Invasive fungal infections in patients with chronic granulomatous disease. *Adv Exp Med Biol*. 2013; 764:27-55.

5. Moskaluk CA, Pogrebniak HW, Pass HI, Gallin JI, Travis WD. Surgical pathology of the lung in chronic granulomatous disease. *Am J Clin Pathol*. 1994;102(5):684-691.

6. Singel KL, Segal BH. Neutrophils in the tumor microenvironment: trying to heal the wound that cannot heal. *Immunol Rev*. 2016;273(1):329-343.

7. Morgenstern DE, Gifford MA, Li LL, Doerschuk CM, Dinauer MC. Absence of respiratory burst in X-linked chronic granulomatous disease mice leads to abnormalities in both host defense and inflammatory response to Aspergillus fumigatus. *J Exp Med*. 1997;185(2):207-218.

8. Endo D, Fujimoto K, Hirose R, et al. Genetic phagocyte NADPH oxidase deficiency enhances nonviable Candida albicans-induced inflammation in mouse lungs. *Inflammation*. 2017;40(1):123-135.

9. Segal BH, Han W, Bushey JJ, et al. NADPH oxidase limits innate immune responses in the lungs in mice. *PLoS One*. 2010;5(3):e9631.

10. Song Z, Huang G, Chiquetto Paracatu L, et al. NADPH oxidase controls pulmonary neutrophil infiltration in the response to fungal cell walls by limiting LTB4. *Blood*. 2020;135(12):891-903.

11. Eyles JL, Roberts AW, Metcalf D, Wicks IP. Granulocyte colony-stimulating factor and neutrophils—forgotten mediators of inflammatory disease. *Nat Clin Pract Rheumatol*. 2006;2(9):500-510.

12. Nemeth T, Mocsai A. Feedback amplification of neutrophil function. *Trends Immunol*. 2016;37(6):412-424.

13. Tecchio C, Micheletti A, Cassatella MA. Neutrophil-derived cytokines: facts beyond expression. *Front Immunol*. 2014;5:508.

14. Ai Z, Udalova IA. Transcriptional regulation of neutrophil differentiation and function during inflammation. *J Leukoc Biol*. 2020;107(3):419-430.

15. Grieshaber-Bouyer R, Radtke FA, Cunin P, et al. The neutrotime transcriptional signature defines a single continuum of neutrophils across biological compartments. *Nat Commun*. 2021;12(1):2856.

16. Khoyratty TE, Ai Z, Ballesteros I, et al. Distinct transcription factor networks control neutrophil-driven inflammation. *Nat Immunol*. 2021;22(9): 1093-1106.

17. Xie X, Shi Q, Wu P, et al. Single-cell transcriptome profiling reveals neutrophil heterogeneity in homeostasis and infection. *Nat Immunol*. 2020;21(9):1119-1133.

18. Manz MG, Boettcher S. Emergency granulopoiesis. *Nat Rev Immunol*. 2014;14(5):302-314.

19. Martin KR, Wong HL, Witko-Sarsat V, Wicks IP. G-CSF - a double edge sword in neutrophil mediated immunity. *Semin Immunol*. 2021;54:101516.

20. Yvan-Charvet L, Ng LG. Granulopoiesis and neutrophil homeostasis: a metabolic, daily balancing act. *Trends Immunol*. 2019;40(7):598-612.

21. Ng LG, Ostuni R, Hidalgo A. Heterogeneity of neutrophils. *Nat Rev Immunol*. 2019;19(4):255-265.

22. Grieshaber-Bouyer R, Nigrovic PA. Neutrophil heterogeneity as therapeutic opportunity in immune-mediated disease. *Front Immunol*. 2019;10:346.

23. Hedrick CC, Malanchi I. Neutrophils in cancer: heterogeneous and multifaceted. *Nat Rev Immunol*. 2021;22(3):173-187.

24. Silvestre-Roig C, Hidalgo A, Soehnlein O. Neutrophil heterogeneity: implications for homeostasis and pathogenesis. *Blood*. 2016;127(18):2173-2181.

25. Hellebrekers P, Vrisekoop N, Koenderman L. Neutrophil phenotypes in health and disease. *Eur J Clin Invest*. 2018;48(Suppl 2):e12943.

26. Han W, Li H, Cai J, et al. NADPH oxidase limits lipopolysaccharide-induced lung inflammation and injury in mice through reduction-oxidation regulation of NF-kappaB activity. *J Immunol*. 2013;190(9):4786-4794.

27. Yoo DG, Paracatu LC, Xu E, Lin X, Dinauer MC. NADPH oxidase limits collaborative pattern-recognition receptor signaling to regulate neutrophil cytokine production in response to fungal pathogen-associated molecular patterns. *J Immunol*. 2021;207(3):923-937.

28. Warnatsch A, Tsourouktsoglou TD, Branzk N, et al. Reactive oxygen species localization programs inflammation to clear microbes of different size. *Immunity*. 2017;46(3):421-432.

29. Trevelin SC, Dos Santos CX, Ferreira RG, et al. Apocynin and Nox2 regulate NF-kappaB by modifying thioredoxin-1 redox-state. *Sci Rep*. 2016;6: 34581.

30. de Luca A, Smeekens SP, Casagrande A, et al. IL-1 receptor blockade restores autophagy and reduces inflammation in chronic granulomatous disease in mice and in humans. *Proc Natl Acad Sci U S A*. 2014;111(9):3526-3531.

31. Meissner F, Seger RA, Moshous D, Fischer A, Reichenbach J, Zychlinsky A. Inflammasome activation in NADPH oxidase defective mononuclear phagocytes from patients with chronic granulomatous disease. *Blood*. 2010;116(9):1570-1573.

32. van de Veerdonk FL, Smeekens SP, Joosten LA, et al. Reactive oxygen species-independent activation of the IL-1beta inflammasome in cells from patients with chronic granulomatous disease. *Proc Natl Acad Sci U S A*. 2010;107(7):3030-3033.

33. van Bruggen R, Koker MY, Jansen M, et al. Human NLRP3 inflammasome activation is Nox1-4 independent. *Blood*. 2010;115(26):5398-5400.

34. Bagaitkar J, Pech NK, Ivanov S, et al. NADPH oxidase controls neutrophilic response to sterile inflammation in mice by regulating the IL-1alpha/G-CSF axis. *Blood*. 2015;126(25):2724-2733.

35. Ligeti E, Geiszt M. CGD: less is more. *Blood*. 2020;135(12):883-884.

36. Geiszt M, Kapus A, Nemet K, Farkas L, Ligeti E. Regulation of capacitative Ca2+ influx in human neutrophil granulocytes. Alterations in chronic granulomatous disease. *J Biol Chem*. 1997;272(42):26471-26478.

37. Sadik CD, Luster AD. Lipid-cytokine-chemokine cascades orchestrate leukocyte recruitment in inflammation. *J Leukoc Biol*. 2012;91(2):207-215.

38. Pollock JD, Williams DA, Gifford MA, et al. Mouse model of X-linked chronic granulomatous disease, an inherited defect in phagocyte superoxide production. *Nat Genet*. 1995;9(2):202-209.

39. Xue X, Pech NK, Shelley WC, Srour EF, Yoder MC, Dinauer MC. Antibody targeting KIT as pretransplantation conditioning in immunocompetent mice. *Blood*. 2010;116(24):5419-5422.

40. Mantovani A, Dinarello CA, Molgora M, Garlanda C. Interleukin-1 and related cytokines in the regulation of inflammation and immunity. *Immunity*. 2019;50(4):778-795.

41. Gabay C, Lamacchia C, Palmer G. IL-1 pathways in inflammation and human diseases. *Nat Rev Rheumatol*. 2010;6(4):232-241.

42. Fuchs A, Monlish DA, Ghosh S, et al. Trauma induces emergency hematopoiesis through IL-1/MyD88-dependent production of G-CSF. *J Immunol*. 2019;202(10):3020-3032.

43. Malengier-Devlies B, Metzemaekers M, Wouters C, Proost P, Matthys P. Neutrophil homeostasis and emergency granulopoiesis: the example of systemic juvenile idiopathic arthritis. *Front Immunol*. 2021;12:766620.

44. Mayle A, Luo M, Jeong M, Goodell MA. Flow cytometry analysis of murine hematopoietic stem cells. *Cytometry A*. 2013;83(1):27-37.

45. Satake S, Hirai H, Hayashi Y, et al. C/EBPbeta is involved in the amplification of early granulocyte precursors during candidemia-induced "emergency" granulopoiesis. *J Immunol*. 2012;189(9):4546-4555.

46. Evrard M, Kwok IWH, Chong SZ, et al. Developmental analysis of bone marrow neutrophils reveals populations specialized in expansion, trafficking, and effector functions. *Immunity*. 2018;48(2):364-379 e368.

47. Luo W, Friedman MS, Shedden K, Hankenson KD, Woolf PJ. GAGE: generally applicable gene set enrichment for pathway analysis. *BMC Bioinformatics*. 2009;10:161.

48. Liberzon A, Birger C, Thorvaldsdottir H, Ghandi M, Mesirov JP, Tamayo P. The Molecular Signatures Database (MSigDB) hallmark gene set collection. *Cell Syst*. 2015;1(6):417-425.

49. Chou RC, Kim ND, Sadik CD, et al. Lipid-cytokine-chemokine cascade drives neutrophil recruitment in a murine model of inflammatory arthritis. *Immunity*. 2010;33(2):266-278.

50. Mohammadi N, Midiri A, Mancuso G, et al. Neutrophils directly recognize group B streptococci and contribute to interleukin-1beta production during infection. *PLoS One*. 2016;11(8):e0160249.

51. Karmakar M, Katsnelson M, Malak HA, et al. Neutrophil IL-1beta processing induced by pneumolysin is mediated by the NLRP3/ASC inflammasome and caspase-1 activation and is dependent on K+ efflux. *J Immunol*. 2015;194(4):1763-1775.

52. Sun Y, Abbondante S, Karmakar M, et al. Neutrophil caspase-11 is required for cleavage of caspase-1 and secretion of IL-1beta in Aspergillus fumigatus infection. *J Immunol*. 2018;201(9):2767-2775.

53. Patankar YR, Mabaera R, Berwin B. Differential ASC requirements reveal a key role for neutrophils and a noncanonical IL-1beta response to Pseudomonas aeruginosa. *Am J Physiol Lung Cell Mol Physiol*. 2015;309(8):L902-913.

54. Karmakar M, Sun Y, Hise AG, Rietsch A, Pearlman E. Cutting edge: IL-1beta processing during Pseudomonas aeruginosa infection is mediated by neutrophil serine proteases and is independent of NLRC4 and caspase-1. *J Immunol*. 2012;189(9):4231-4235.

55. Cho JS, Guo Y, Ramos RI, et al. Neutrophil-derived IL-1beta is sufficient for abscess formation in immunity against Staphylococcus aureus in mice. *PLoS Pathog*. 2012;8(11):e1003047.

56. Karmakar M, Minns M, Greenberg EN, et al. N-GSDMD trafficking to neutrophil organelles facilitates IL-1beta release independently of plasma membrane pores and pyroptosis. *Nat Commun*. 2020;11(1):2212.

57. Kremserova S, Nauseef WM. Frontline science: staphylococcus aureus promotes receptor-interacting protein kinase 3- and protease-dependent production of IL-1beta in human neutrophils. *J Leukoc Biol*. 2019;105(3):437-447.

58. Tourneur L, Witko-Sarsat V. Inflammasome activation: neutrophils go their own way. *J Leukoc Biol*. 2019;105(3):433-436.

59. Salina ACG, Brandt SL, Klopfenstein N, et al. Leukotriene B4 licenses inflammasome activation to enhance skin host defense. *Proc Natl Acad Sci U S A*. 2020;117(48):30619-30627.

60. Capucetti A, Albano F, Bonecchi R. Multiple roles for chemokines in neutrophil biology. *Front Immunol*. 2020;11:1259.

61. Drummond RA, Franco LM, Lionakis MS. Human CARD9: a critical molecule of fungal immune surveillance. *Front Immunol*. 2018;9:1836.

62. Cain DW, Snowden PB, Sempowski GD, Kelsoe G. Inflammation triggers emergency granulopoiesis through a density-dependent feedback mechanism. *PLoS One*. 2011;6(5):e19957.

63. Altmeier S, Toska A, Sparber F, Teijeira A, Halin C, LeibundGut-Landmann S. IL-1 coordinates the neutrophil response to C. albicans in the oral mucosa. *PLoS Pathog*. 2016;12(9):e1005882.

64. Liao YC, Wu SY, Huang YF, et al. NOX2-deficient neutrophils facilitate joint inflammation through higher pro-inflammatory and weakened immune checkpoint activities. *Front Immunol*. 2021;12:743030.

65. Tak T, Wijten P, Heeres M, et al. Human CD62L(dim) neutrophils identified as a separate subset by proteome profiling and in vivo pulse-chase labeling. *Blood*. 2017;129(26):3476-3485.

66. Leliefeld PHC, Pillay J, Vrisekoop N, et al. Differential antibacterial control by neutrophil subsets. *Blood Adv*. 2018;2(11):1344-1355.

67. van Grinsven E, Textor J, Hustin LSP, Wolf K, Koenderman L, Vrisekoop N. Immature neutrophils released in acute inflammation exhibit efficient migration despite incomplete segmentation of the nucleus. *J Immunol*. 2019;202(1):207-217.

68. Bongers SH, Chen N, van Grinsven E, et al. Kinetics of neutrophil subsets in acute, subacute, and chronic inflammation. *Front Immunol*. 2021;12: 674079.

69. Tsuda Y, Takahashi H, Kobayashi M, Hanafusa T, Herndon DN, Suzuki F. Three different neutrophil subsets exhibited in mice with different susceptibilities to infection by methicillin-resistant Staphylococcus aureus. *Immunity*. 2004;21(2):215-226.

70. Zhu YP, Eggert T, Araujo DJ, Vijayanand P, Ottensmeier CH, Hedrick CC. CyTOF mass cytometry reveals phenotypically distinct human blood neutrophil populations differentially correlated with melanoma stage. *J Immunother Cancer*. 2020;8(2):e000473.

71. Wang H, Aloe C, McQualter J, et al. G-CSFR antagonism reduces mucosal injury and airways fibrosis in a virus-dependent model of severe asthma. *Br J Pharmacol*. 2021;178(8):1869-1885.

72. Lee MC, McCubbin JA, Christensen AD, et al. G-CSF receptor blockade ameliorates arthritic pain and disease. *J Immunol*. 2017;198(9):3565-3575.

73. Scalzo-Inguanti K, Monaghan K, Edwards K, et al. A neutralizing anti-G-CSFR antibody blocks G-CSF-induced neutrophilia without inducing neutropenia in nonhuman primates. *J Leukoc Biol*. 2017;102(2):537-549.